

# Towards ultra-large area vascular contrast skin imaging using multi-MHz-OCT

Madita Göb<sup>1</sup>, Sazgar Burhan<sup>1</sup>, Simon Lotz<sup>1</sup>, Robert Huber<sup>1</sup>

<sup>1</sup>Institut für Biomedizinische Optik, Universität zu Lübeck, Peter-Monnik-Weg 4, 23562 Lübeck, Germany

## 1. INTRODUCTION

Optical coherence tomography (OCT) as a non-invasive, three-dimensional imaging technique has a growing impact on diagnostics of skin diseases. For clinical application and with respect to bulk motion artifacts the image acquisition time is a crucial factor. With the advent of multi-Megahertz Fourier Domain Mode Locked (FDML) lasers, the imaging speed of OCT systems was dramatically increased [1]. Besides high temporal resolution for live 3D imaging at video volume update rates [2], the high A-scan rate of our home-built 3.3 MHz-OCT system is also beneficial for large area scanning. To facilitate large area OCT imaging, we recently built a motorized and controllable XYZ-positioning stage and demonstrated some first preliminary simple mosaicking OCT images of *in vivo* skin [3].

In this paper, we demonstrate an advanced scanning mode, where we operate the X-Y-galvanometer scanner and the motorized stage synchronously by a custom hardware trigger circuitry. Instead of scanning several volumes step-by-step with the stage moving in between, the motorized XYZ-stage is driven at constant speed, synchronously to the X-scanner of the OCT system, allowing the acquisition of coherent ultra-large areas without stitching artifacts. We demonstrate different large area OCT images and discuss the limits and challenges of the technique, especially considering the high OCT line rate. Further, the application for *in vivo* OCT-based angiography (OCTA) of human skin will be discussed. In contrast to established OCTA methods based on repeated frames or volumes [4, 5], an advanced scanning protocol was developed. In this mode, the Y-galvanometer axis scanner is driven in a repetitive sawtooth pattern fully synchronized to the movement of the linear stage to obtain multiple measurements at each position. Similar to the effective scanning protocol of Hsu et al, this allows to effectively leverage the full potential of multi-MHz OCT for vascular contrast imaging [6]. However, for exact revisitations, it is necessary to control the position of the motorized stage on a sub-micrometer scale. At the same time, fast imaging requires very high stepping speed of the stage. This extreme precision at high speed is very challenging and we face several problems with wobble and non-linear stage movements. Thus, in this work we will analyze these obstacles in detail, discuss possible solutions and show preliminary OCT images.

## 2. METHODS

All data shown in this work was acquired using a home-built OCT system based on an FDML laser source with a center wavelength of 1310 nm and an effective A-scan rate of 3.3 MHz. We used a spectral bandwidth of ~100 nm, the incident power on the sample was 25 mW and OCT data were acquired at 4 GS/s with a sample depth of 12 bit (AlazarTech, ATS9373, Canada). The beam delivery system consists of a pair of galvanometer mirror scanners (Cambridge Technology, 6215H, USA) operated in unidirectional scanning mode and a simple 50 mm scan lens.

The custom built motorized XYZ-positioning stage is based on the combination of three linear stages that allow a scan area of approximately 20x20x20 cm. For precise positioning, stepper motors (TRINAMIC Motion Control GmbH, QSH4218-51-10-049-10000-AT, Germany) and the corresponding triple axis stepper motor driver board (TRINAMIC Motion Control GmbH, TMCM-3110-TMCL, Germany) are used. A control software (LabVIEW, National Instruments, USA) was developed that enables automated scan head positioning synchronized to our OCT imaging software. The software allows to use the stage in different imaging modes, such as the mosaicking mode, interoperation mode and stepped interoperation mode.

For mosaicking, the motorized scan head is moved according to the specific lateral field of view (FOV) of the OCT volume (Figure 1). In this first mode the stage is not synchronized to the scanners and is triggered to move to the next position while writing the OCT raw data. In the mosaicking OCTA mode, vascular contrast is calculated by intervolumetric speckle contrast and therefore five volumes per position are acquired. Following the OCT image processing, stitching was performed using the Microsoft Image Composite Editor (Microsoft ICE, Microsoft Research, USA). For the second mode, interoperation mode of stage and scanners, the interface of the OCT imaging software to the scanner driver board was extended to include triggers to the stepper motor driver board (Figure 2). This allows precise positioning of the stage down to 535 nm steps (with the currently implemented gear ratio) synchronized with the fast galvanometer scanner in X-direction, while the slow axis scanner is replaced by the stage. Thus, larger lateral FOVs exceeding the FOV possible by two scanners only can be achieved. The third mode, the stepped interoperation mode, also includes the slow galvanometer scanner in Y-direction (Figure 4). It is programmed to move in the same direction as the stage and step back to a certain position after a specific time interval for dynamic speckle contrast calculation.

To evaluate the performance of each mode a human hand *in vivo*, a stripboard and a grid distortion target (Thorlabs, R1L3S3P, USA) were imaged and subsequently analyzed. All *in vivo* experiments of human hands are conducted on voluntarily basis by experts of our group and approved by the Ethics Committee of the University of Lübeck.

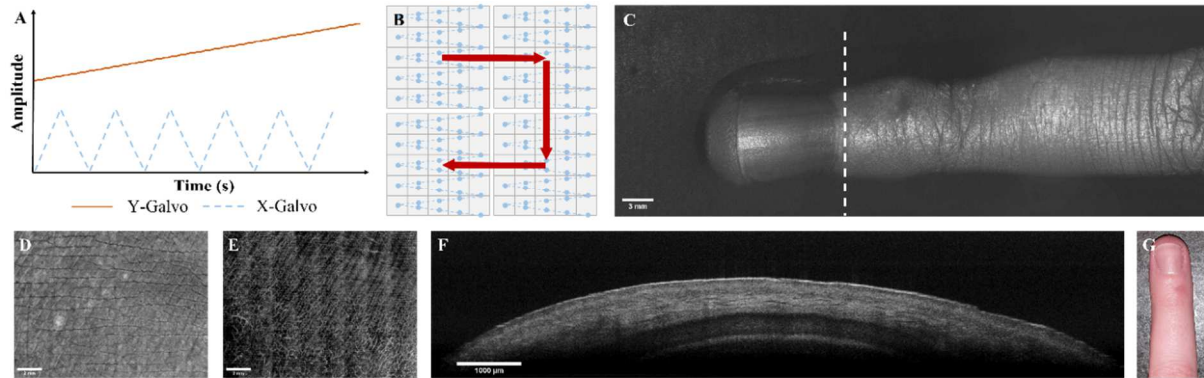


**Figure 1** Mosaicking mode. (A) Waveform signals for the scanning optics and (B) the resulting scan pattern. (C) Stitched enface OCT intensity image of a finger composed of 6x2 tiles with (F) corresponding stitched depth scan at the marked position. (G) Photo of the finger. (D) OCT intensity image of the palm composed of 8x6 tiles and (E) the corresponding stitched vascular contrast mode OCT image of the same dataset.

### 3. RESULTS AND DISCUSSION

The mosaicking mode is visualized in Figure 1. With this mode, large FOV OCT images of an entire finger can be realized (Figure 1C). Stitching was performed in two planes with 23 % overlap in each direction. In the B-scan view (Figure 1F) minor stitching artifacts are visible, but the enface projections appear seamless. To demonstrate a large area OCTA image, 48 OCT volumes of the palm with five-time repetition were acquired. Subsequently, the enface projections of the intensity images (Fig. 1D) as well as the speckle contrast (Fig. 1E) in different depths were calculated and stitched together. While the stitched intensity image does not show any stitching artifacts, some vignetting is visible in the vascular contrast image. Further, the image quality of the contrast OCT image is affected by the tilt of the cover glass on top of the palm and minor motion artifacts.

To avoid these artifacts and to increase the overall acquisition speed, the interoperation mode was developed whose scanning pattern is visualized in Figure 2. As depicted in Figure 2C, this mode enables coherent large area acquisitions. In this particular example each tile is 4.5x18 mm<sup>2</sup>. The software also features mosaicking scan patterns by adjusting the stage direction for the interoperation mode and interim stage steps in X-direction.

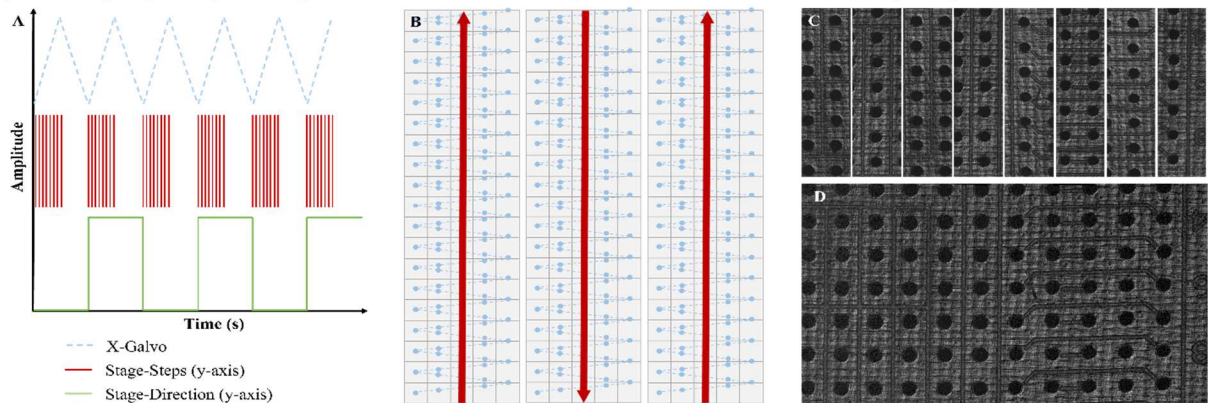


**Figure 2** Interoperation mode with movable stage as slow scanning axis. (A) Waveform and trigger signals for the scanning optics and stage and (B) the resulting scan pattern. (C) Enface projections of individual large area OCT scans and (D) the resulting stitched OCT image of a stripboard.

We compared the image quality of the interoperation mode, using the stage as the slow scanning axis to the conventional scanning mode and noticed several artifacts, exemplarily displayed in Figure 3B. In both directions non-uniform movements could be analyzed. The non-linear movement in X-direction could be assigned to non-linear responses of the fast galvo scanner and be solved by driving the galvo with a sinusoidal instead of ramp waveform. Considering non-uniform movements of the stage (visible in the OCT images non-uniform height of the squares), we could exclude software and trigger problems after conducting various tests and scrutinizing the setup. Most problems were solved by carefully reassembling selected parts of the stage (Figure 3C).

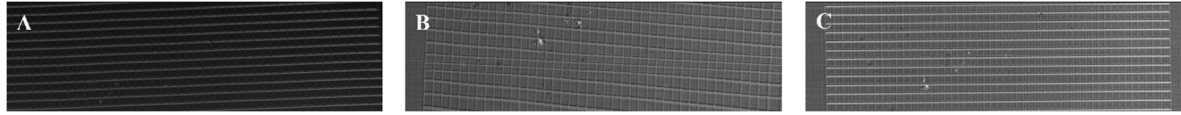


**Figure 3** Comparison of different imaging modes using a 100  $\mu\text{m}$  grid distortion target. (A) Conventional OCT scan using X-Y-galvos. (B) Interoperation mode OCT with non-linear stepping issues. (C) Interoperation mode OCT with optimized stage setup and sinusoidal galvo drive waveform.

Next, the stepped interoperation mode was investigated to be used for interframe based speckle contrast for variable time intervals (Figure 4). The speed of the stage was set to one fourth of the speed of the slow, back-jumping galvanometer scanner to allow at least four revisitations of each spot and thus to calculate vascular contrast of four different timepoints. Unfortunately, in our first trial the revisitation is not precise enough to obtain good vascular contrast without background noise. As visible in the intensity image of the grid in Figure 4C, each spot seems to be revisited after exactly 96 frames (corresponding to 96 pixels in vertical direction). However, when imaging *in vivo* skin, no vascular contrast can be observed in the derived OCTA images (Figure 4E), even though the acquired position in the sample seems to be exactly the same and no blurring is visible in the 4x averaged intensity image (Figure 4D). We will further investigate this problem in order to improve the signal levels.

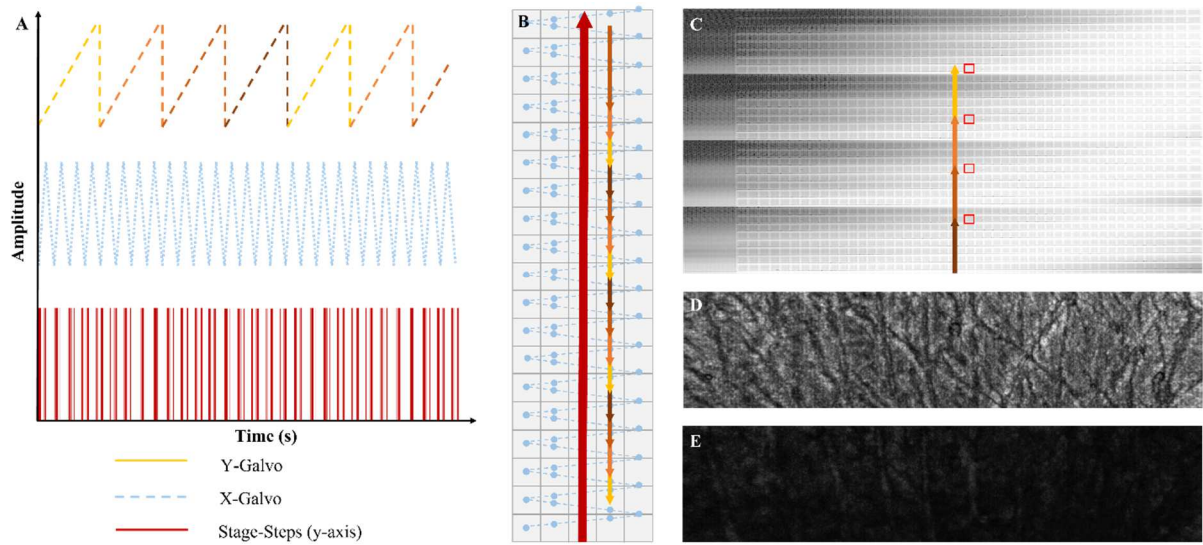


**Figure 4** Stepped interoperation mode with movable stage and X-Y-galvo scanners. (A) Waveform and trigger signals for the scanning optics and stage and (B) the resulting scan pattern with arrows indicating steps in Y-direction. (C) OCT intensity image of a 100  $\mu\text{m}$  grid distortion target with coincident positions labeled. (D) Resulting intensity OCT image of a palm based on 4x averaging of coincident frames. (E) Speckle contrast image of the dataset based on standard deviation values of 4 coincident frames.

#### 4. CONCLUSION AND OUTLOOK

The imaging experiments with the motorized stage show promising first results for ultra-large area MHz-OCT. However, testing the advanced scanning protocol incorporating standard scan optics, scanners and the movable stage revealed many obstacles that we will further investigate to achieve high quality, fast ultra-large FOV OCTA images.

#### REFERENCES

1. W. Wieser, B. Biedermann, T. Klein, C. Eigenwillig, and R. Huber, "Multi-Megahertz OCT: High quality 3D imaging at 20 million A-scans and 4.5 GVoxels per second," *Opt. Express* **18**, 14685-14704 (2010).
2. W. Wieser, W. Draxinger, T. Klein, S. Karpf, T. Pfeiffer, and R. Huber, "High definition live 3D-OCT in vivo: design and evaluation of a 4D OCT engine with 1 GVoxel/s," *Biomed. Opt. Express* **5**, 2963-2977 (2014).
3. M. Göb, S. Burhan, W. Draxinger, J. P. Kolb, and R. Huber, "Towards Densely Sampled Ultra-Large Area Multi-MHz-OCT for in Vivo Skin Measurements Beyond 1  $\text{cm}^2/\text{sec}$ ," in *European Conference on Biomedical Optics, EW3C.4* (Munich, 2021).
4. A. J. Deegan, F. Talebi-Liasi, S. Song, Y. Li, J. Xu, S. Men, M. M. Shinohara, M. E. Flowers, S. J. Lee, and R. K. Wang, "Optical coherence tomography angiography of normal skin and inflammatory dermatologic conditions," *Lasers in Surgery and Medicine* **50**, 183-193 (2018).
5. S. Men, J. M. Wong, E. J. Welch, J. Xu, S. Song, A. J. Deegan, A. Ravichander, B. Casavant, E. Berthier, and R. K. Wang, "OCT-based angiography of human dermal microvascular reactions to local stimuli: Implications for increasing capillary blood collection volumes," *Lasers in Surgery and Medicine* **50**, 908-916 (2018).
6. D. Hsu, J. H. Kwon, A. Athwal, Y. Miao, Y. Jian, M. Sarunic, and M. J. Ju, *Effective scanning protocol for optical coherence tomography and angiography using a 1.6 MHz Fourier domain mode-locked laser source* (SPIE, 2021).